3-24-2012

A phase-field model for phase transformations in glass-forming alloys

Tao Wang
Iowa State University, taowang@ameslab.gov

Ralph E. Napolitano
Iowa State University, ren1@iastate.edu

A phase-field model for phase transformations in glass-forming alloys

Abstract
A phase-field model is proposed for phase transformations in glass-forming alloys. The glass transition is introduced as a structural relaxation, and the competition between the glass and crystalline phases is investigated. The simulations are performed for Cu-Zr alloys, employing thermodynamic and kinetic parameters derived from reported thermodynamic modeling and molecular dynamics simulation results,[1–3] respectively. Four distinct phase fields are treated with a multi-phase-field approach, representing the liquid/glass, $Cu_{10}Zr_7$, CuZr, and $CuZr_2$ phases. In addition, a continuum-field method is applied to the liquid to accommodate the liquid–glass transformation. The combined phase-field approach is used to investigate the glass formation tendency, and critical cooling rates are estimated and compared with the reported experimental values.

Keywords
Ames Laboratory

Disciplines
Ceramic Materials

Comments
This article is from *Metallurgical and Materials Transactions A* 43 (2012): 2662, doi:10.1007/s11661-012-1136-2. Posted with permission.

A Phase-Field Model for Phase Transformations in Glass-Forming Alloys

TAO WANG and RALPH E. NAPOLITANO

A phase-field model is proposed for phase transformations in glass-forming alloys. The glass transition is introduced as a structural relaxation, and the competition between the glass and crystalline phases is investigated. The simulations are performed for Cu-Zr alloys, employing thermodynamic and kinetic parameters derived from reported thermodynamic modeling and molecular dynamics simulation results,[1–3] respectively. Four distinct phase fields are treated with a multi-phase-field approach, representing the liquid/glass, $Cu_{10}Zr_7$, CuZr, and $CuZr_2$ phases. In addition, a continuum-field method is applied to the liquid to accommodate the liquid–glass transformation. The combined phase-field approach is used to investigate the glass formation tendency, and critical cooling rates are estimated and compared with the reported experimental values.

DOI: 10.1007/s11661-012-1136-2

I. INTRODUCTION

WITH extensive potential applications arising from a remarkable range of mechanical, physical, and chemical properties, the growing class of metallic alloys continue to generate scientific and technological interest; these alloys are known as bulk metallic glasses (BMGs) because they can be quenched to glassy solids in relatively thick sections. New BMG alloy development has relied heavily on experimental exploration, and the attempts to correlate glass-forming tendency with fundamental thermodynamic properties have not led to a predictive ability in any general sense.[4–7] As a complement to the experiment, computational methods may offer powerful avenues for studying glass formation and other properties of glass-forming alloys.[8] Indeed, both classical and *ab initio* molecular dynamics (MD) methods have provided substantial fundamental gains related to the structural aspects of the glass transition along with insights into the influence of alloy chemistry on the glass-forming tendency in several alloy systems (*e.g.*, Al-Mg,[9] Cu-Zr,[1,10] Ni-Zr,[11,12] Ag-Ni-Zr,[13] and Ca-Mg-Zn[14]). Focusing mainly on the short- and medium-range structure that persists over a few coordination shells, these methods have shown that the glass transition may be associated with (1) the dominance of specific noncrystalline motifs in the liquid and (2) the emergence of a fine network structure of well-ordered but noncrystalline material, where the liquid-like material is divided into small cellular volumes.[15,16] With these advancements related to the atomistic nature of the glass transition as well as the thermodynamic and kinetic properties of undercooled metallic liquids, new computational methods are required to connect the basic mechanisms and properties to bulk behavior. Specifically, models are required to predict the glass transition on rapid cooling of the melt and the simultaneous competition between the various crystalline phases for which solidification may be highly driven. Such models should account for the cooling rate effects that influence strongly the atomistic structure, the related properties of the undercooled liquid, and the associated transition kinetics. The relevant length and time scales are too large for the direct application of MD methods,[17,18] and we consider in this article the application of a phase-field approach, which has been used widely to simulate many types of phase transformation at the mesoscale or microstructural level.[19,20]

The characteristic feature of a phase-field treatment is that the local free-energy density (or some other thermodynamic potential) is defined in terms of a set of field variables that together yield the local potential minima at specific states. In addition, the field variables, the free energy density, and all the gradients are continuous over the spatial domain. The transformation in the system is described by evolving the phase variables toward a minimum in the total free energy functional (F). By drawing model parameters from the reliable thermodynamic and the kinetic databases, the phase-field approach can provide trustworthy predictions for the structural dynamics of the corresponding system.[21,22]

The phase-field models have been applied successfully to various microstructural transformations, with the continuum-field (CF)[20,23,24] and multi-phase-field (MPF)[25,26] approaches being prevalent. In the CF approach, the phase variable is chosen to vary between two possible limits, each representing a specific state. Thus, a simple transition between two states, not limited as a phase transformation, can be represented with a single phase variable, typically coupled with a tempera-

TAO WANG, Assistant Scientist, is with the Division of Materials Sciences and Engineering, Ames Laboratory, U.S. Department of Energy, Ames, IA 50011. Contact e-mail: taowang@iastate.edu RALPH E. NAPOLITANO, Scientist, is with the Division of Materials Sciences and Engineering, Ames Laboratory, U.S. Department of Energy, is also a Professor with the Department of Materials Science and Engineering, Iowa State University, Ames, IA 50011.

Manuscript submitted April 30, 2011.
Article published online March 24, 2012

ture and/or composition field and the associated transport equations. The CF approach has been applied with great success in the prediction of solidification dynamics[27–30] and solid-state microstructure evolution.[20,31–33] In the MPF approach, each phase is assigned a different phase variable, which varies between two limits indicating the presence or absence of that particular phase. Thus, the sum of all the phase fields is constrained to be unity at any position in the system.[34] The MPF approach has been applied to the phenomena involving many different phases[35,36] and/or many grains of the same phase.[37,38]

Despite the broad scope of phase-field applications,[19,20,39–41] glass-involved transformations have not been modeled widely. Few reports[42,43] are available, and the treatment of the glassy phase is limited. For example, Kawaguchi and Onda[42] used a CF approach to describe the liquid-crystal-amorphous phase transformations in optical memory devices. Two artificial phase fields were introduced: "stiffness" to distinguish solid and liquid phases, and "molecular orientation" to separate the crystal and amorphous states of the solid phase.[42] Although the model predicted the phase transitions successfully at rapid and slow cooling rates, it cannot be extended to the systems readily with multiple crystalline phases.

Because the liquid–glass transition may proceed as a first- or second-order transition and may be competing with multiple crystalline phases, we propose a hybrid CF-MPF formulation for glass-forming systems, where the structural variation associated with the liquid–glass transition is treated using a CF phase variable, and the different specific crystalline phases are described as discrete entities in a MPF formulation. With this approach, we model the Cu-Zr system as an example and examine the competition between the various crystalline phases that may be driven to nucleate from an undercooled liquid simultaneous with the noncrystalline ordering that may occur in the liquid as it is cooled through the glass transition temperature T_g.

II. MODEL FORMULATION

In the current formulation, we describe the overall mesoscale assemblage involving m specific phases using the field variables $\bar{\phi} = (\phi_1, \phi_2, \ldots, \phi_m)$, where each ϕ_i may vary between the absence ($\phi_i = 0$) or the presence ($\phi_i = 1$) of that phase, under the constraint that $\sum_i \phi_i = 1$ everywhere in the domain. We also employ the field variable η to represent the variation between the liquid ($\eta = 0$) and the glass ($\eta = 1$) in any material of noncrystalline character and include the concentrations of n solutes, $\bar{c} = (c_1, c_2, \ldots, c_n)$. The relevant free energy density is

$$f = \sum\nolimits_i \phi_i f_i + \sum\nolimits_{i<j} w_{ij}\phi_i^2\phi_j^2 + w_\eta \eta^2(1-\eta)^2 + W_{ex} \quad [1]$$

The first term on the right-hand side of the equation describes the chemical contribution, and f_i is the free-energy density of each separate phase. Both w_{ij} and w_η are positive coefficients, and W_{ex} is a general coupling term to describe the interactions between the $\bar{\phi}$ and η fields. The corresponding free energy functional is

$$F = \int_V \left[f + \sum\nolimits_{i<j} \frac{\varepsilon_{ij}^2}{2}\left(\phi_i \nabla\phi_j - \phi_j \nabla\phi_i\right)^2 + \frac{\beta}{2}(\nabla\eta)^2 \right] dV \quad [2]$$

where ε^2 and β are the gradient energy coefficients for $\bar{\phi}$ and η, respectively. The temporal evolution each phase field is given by the Cahn-Hillard and Allen-Cahn equations

$$\frac{\partial \phi_i}{\partial t} = -L_{ij}\frac{\delta F}{\delta \phi_j} \quad [3]$$

$$\frac{\partial \eta}{\partial t} = -L_\eta \frac{\delta F}{\delta \eta} \quad [4]$$

$$\frac{\partial c_k}{\partial t} = \nabla \cdot \left(M_{kl} \nabla \frac{\delta F}{\delta c_l} \right) \quad [5]$$

where M and L are related to atom or interface mobility.

If we constrain the η field to be zero everywhere, then the current model reduces to the MPF model and can be used to simulate multiphase solidification without glass formation. Relaxing this constraint and perturbing the η field with a Gaussian "noise" at every time step, we allow the glass transition to occur, depending on the energetic barrier imparted by the magnitude of the double-well coefficient, w_η, in Eq. 1. Figure 1 shows three examples of simulated structures, each resulting from rapidly quenching the liquid phase through T_g, representing systems with a large, small, or zero energy barrier for the liquid–glass transition. The results show that the transition can be modeled reasonably for this full spectrum between a classic activated nucleation/growth process (case 1) to a zero-barrier spinodal type of transition (case 3).

III. SIMULATIONS OF TRANSITIONS IN THE Cu-Zr SYSTEM

We now apply the model to phase transition in the Cu-Zr binary considering four distinct phases: liquid/glass (ϕ_0), $Cu_{10}Zr_7$ (ϕ_1), CuZr (ϕ_2), and $CuZr_2$ (ϕ_3), and the structural relaxation (glass transition) described by η is also considered.*

*The phase field η, which is taken generically as a measure of noncrystalline order, can be connected with one or more characteristics of the transformation for any particular system. For example, in the case of Cu-Zr, it is reasonable to relate that value of η to the number of icosahedral clusters, the extent (number of coordination shells) of medium range order, and the extent of network development, as discussed previously.

Under these conditions ($m = 4$, $n = 1$), the chemical part of the local free energy density f_c is given by

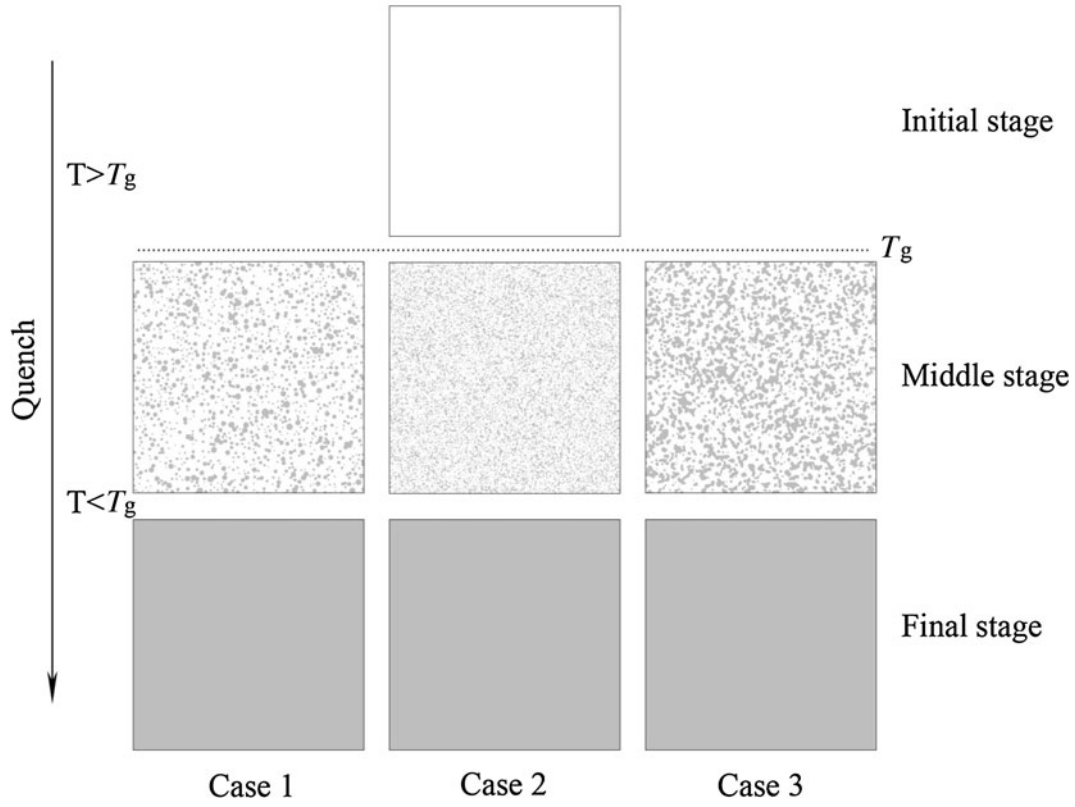

Fig. 1—Structural relaxation in a test system. The white and gray colors indicate the two states of the relaxation, *i.e.*, $\eta = 0$ and $\eta = 1$, respectively. T_g is the transition temperature, and different cases refer to different assumptions. The artificial parameters used for this simulation are: $f_c(\eta = 0) - f_c(\eta = 1) = 4$kJ/mol, $\beta = 4 \times 10^{-11}$J/m, $w_\eta = 4 \times 10^8$J/m^3, and $L_\eta = 0.1$m^3/s/J. The values of β and w_η in case 2 are decreased by an order of magnitude to represent a small energy barrier.

$$\begin{aligned} f_c(c, T, \bar{\phi}, \eta) &= \sum_{i=0}^{3} \phi_i f_i(c, T, \eta) \\ &= \phi_0 \left[f_0(c, T, 0) + h(\eta) \Delta f^{SR}(c, T) \right] \\ &\quad + \sum_{i=1}^{3} \phi_i f_i(c, T) \end{aligned} \quad [6]$$

where $\Delta f^{SR}(c, T) = f_0(c, T, 1) - f_0(c, T, 0)$ and the function $h(\eta) = \eta^3(10 - 15\eta + 6\eta^2)$ is used to interpolate between the free energies of liquid and glass. In this work, we define the coupling term W_{ex} in Eq. 1 as

$$W_{ex} = w_{ex} \eta^2 \sum_{i \neq 0} \phi_i^2 \quad [7]$$

where w_{ex} is a positive coefficient, indicating the extent of coupling between $\bar{\phi}$ and η.

In summary, the model parameters required for the simulations of phase transition in the Cu-Zr system are the thermodynamic terms f_i and Δf^{SR}, gradient energy coefficients ε^2 and β, coupling coefficients w_{ex}, and kinetic parameters M and L.

Table I. Available Information from the Literature for the $Cu_{50}Zr_{50}$ Alloy

Property	Units	Value	Method
T_m (CuZr-B2)	K (°C)	1323 (1050)	MD[2,44]
		1208 (935)	CalPhaD[3]
T_m ($Cu_{10}Zr_7$)	K (°C)	1160 (887)	CalPhaD[3]
T_m ($CuZr_2$)	K (°C)	1129 (856)	CalPhaD[3]
T_g	K (°C)	700 (427)	Experiment[45]
		685 (412)	Experiment[46]
		587 (314)	Experiment[47]
		666 (393)	Experiment[48]
		715 (442)	MD[2,44]
ΔH_m (CuZr-B2)	kJ/mol	19.4	MD[2,44]
		11.2	CalPhaD[3]
ΔH_m ($Cu_{10}Zr_7$)	kJ/mol	14.3	CalPhaD[3]
ΔH_m ($CuZr_2$)	kJ/mol	13.8	CalPhaD[3]
μ_{100} (L-B2)	m/sK	0.0018	MD[2,44]
μ_{110} (L-B2)	m/sK	0.0026	MD[2,44]

A. *Evaluation of Model Parameters*

Thermodynamic and kinetic data were collected from the literature to determine the model parameters. Table I shows the available information from the literature for $Cu_{50}Zr_{50}$ alloy. The experimental information is limited and the data from different sources are scattered, especially for the glass transition. Therefore, we introduce a small energy barrier for the liquid–glass transition (similar to case 2 in Figure 1), which allows the transition be activated by a low-amplitude "noise" in the η field.

In the current work, the free-energy densities (f_i) of the crystalline and disordered liquid ($\eta = 0$) were computed from recently developed thermodynamic databases for the Cu-Zr system.[3] The low-temperature

liquid free energy is extrapolated directly from the high-temperature behavior, and the free energy of the glass ($\eta = 1$) is obtained by computing the liquid-glass free energy change (Δf^{SR}) as a function of temperature using the model (and parameters for Cu-Zr) reported by Shao[49] and Abe *et al.*,[50] where

$$\Delta f^{SR} = -RT_g \ln(1+\alpha) f(\tau) \quad [8]$$

and where T_g is the glass transition temperature, $\tau = T/T_g$, α is a model parameter related to the amorphization, and $f(\tau)$ the Hillert–Jarl function.[49,50] The resulting free energies are shown in Figure 2 for the $Cu_{50}Zr_{50}$ composition, along with the corresponding enthalpy change associated with the glass transition $\Delta H^{SR} = H_0(\eta = 1) - H_0(\eta = 0)$.

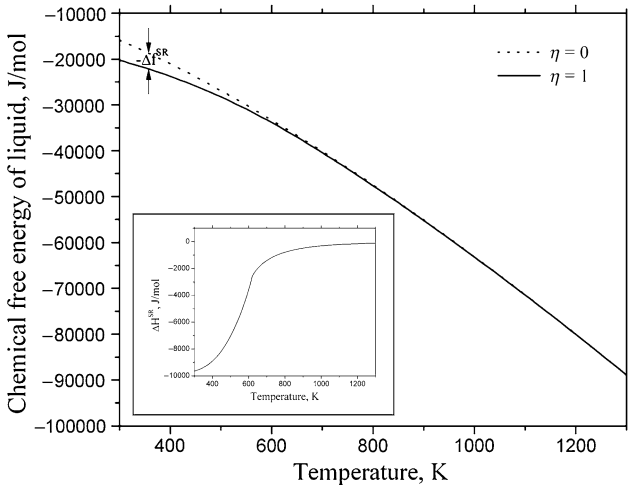

Fig. 2—Chemical free energy description for the liquid $Cu_{50}Zr_{50}$ alloy from the recently developed Cu-Zr thermodynamic databases.[3,50] $\Delta f^{SR} = f_0(\eta = 1) - f_0(\eta = 0)$ and $\Delta H^{SR} = H_0(\eta = 1) - H_0(\eta = 0)$, indicating the changes of free energy and entropy associated with the glass transition, respectively.

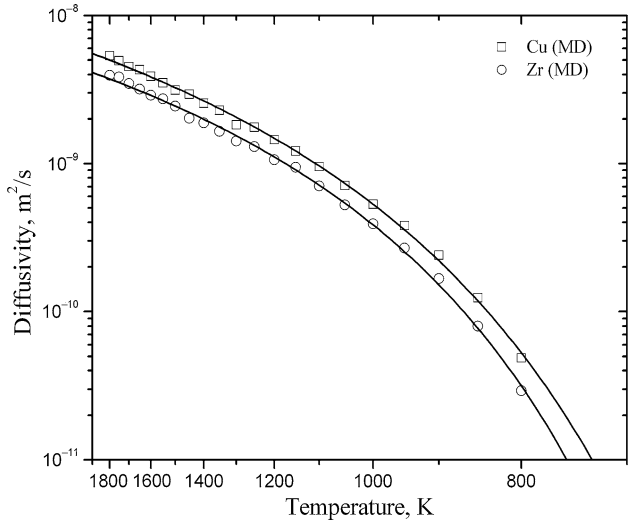

Fig. 3—Diffusivity of Cu and Zr in the liquid $Cu_{50}Zr_{50}$ alloy, where the symbols are from MD simulations,[1] and the solid curves are fitting results under the Vogel–Tammann–Fulcher relation.

The gradient terms are linked physically to interfacial free energies, but there are no experimentally determined liquid/solid interfacial energies ($\gamma^{S/L}$) for Cu-Zr alloys. A commonly used method for predicting $\gamma^{S/L}$ was developed by Turnbull,[51,52] who found that $\gamma^{S/L}$ is proportional to the latent heat of fusion (ΔH_m) with a coefficient $\alpha = 0.45$ for metals. In the current work, the interfacial energies between the liquid and different crystals were estimated by the broken-bond method proposed by Granasy *et al.*,[53] where the structural effects are considered in the correlation of $\gamma^{S/L}$ with the temperature-dependent enthalpy and entropy differences (ΔH and ΔS) between the bulk liquid and crystal phases. At the melting temperature (T_m), with $\Delta H = \Delta H_m$ and $\Delta S = \Delta H_m/T_m$, the correlation between $\gamma^{S/L}$ and ΔH_m suggested by Turnbull[51,52] can be reproduced by Granasy's model,[53] and the coefficient α depends on the crystal structure. For the B_2-CuZr phase, the minimum α is 0.445, which agrees well with Turnbull's value (0.45).

Diffusivity in different each of the phases is required to determine the kinetic coefficients, but no experimental investigation has been reported for the Cu-Zr alloys in the literature. Mendelev *et al.*[2] estimated the self-diffusivity of Cu and Zr in liquid Cu-Zr alloys by MD simulations, which have been adopted in this work. Sun *et al.*[54] studied the atomic structure and diffusion in the $Cu_{60}Zr_{40}$ liquid and glass by MD simulations and found that the amount of pentagonal bipyramids increases sharply in a short temperature range of approximately 200 K (200 °C) above the glass transition temperature T_g, leading to the increasing of the icosahedral and polytetrahedral clusters. A recent *ab initio* molecular dynamics (AIMD) investigation[16] found strong self-aggregation of icosahedral clusters in $Zr_{1-x}Cu_x$ liquids, resulting in a stringlike network that causes a significant kinetic slowdown and then a glass transition. The kinetic slowdown above T_g was also observed from

Table II. Model Parameters for $Cu_{50}Zr_{50}$ Alloy at the Melting Temperature (1208 K [935 °C])

$\varepsilon^2_{13} = 1.1 \times 10^{-9}$ J/m	$w_{01} = 4.2 \times 10^8$ J/m^3	$L_{01} = 0.05$ m^3/s/J
$\varepsilon^2_{13} = 0.7 \times 10^{-9}$ J/m	$w_{02} = 4.1 \times 10^8$ J/m^3	$L_{02} = 0.08$ m^3/s/J
$\varepsilon^2_{03} = 1.2 \times 10^{-9}$ J/m	$w_{03} = 4.7 \times 10^8$ J/m^3	$L_{03} = 0.05$ m^3/s/J
$\varepsilon^2_{12} = 1.0 \times 10^{-10}$ J/m	$w_{12} = 1.0 \times 10^8$ J/m^3	$L_{12} = 0.005$ m^3/s/J
$\varepsilon^2_{13} = 1.0 \times 10^{-10}$ J/m	$w_{13} = 1.0 \times 10^8$ J/m^3	$L_{13} = 0.005$ m^3/s/J
$\varepsilon^2_{23} = 1.0 \times 10^{-10}$ J/m	$w_{23} = 1.0 \times 10^8$ J/m^3	$L_{23} = 0.005$ m^3/s/J
$\beta = 2.6 \times 10^{-12}$ J/m	$w_\eta = 2.5 \times 10^7$ J/m^3	$L_\eta = 1.36$ m^3/s/J
	$w_{ex} = 2.0 \times 10^9$ J/m^3	

Mendelev 's diffusivity data.[44] MD-based data[1] at high temperatures ($T > 800$ K [527 °C]) were adopted in this work for liquid with $\eta = 0$, and the low-temperature values were extrapolated using the Vogel–Tammann–Fulcher relation, as shown in Figure 3. Because the diffusivity is small at low temperatures and the MD data cannot provide reliable conclusions,[44] the diffusivity in glass ($\eta = 1$) is still unknown. Similarly, no data available for diffusion in the crystalline Cu-Zr phases are available, and we simply set the diffusivities in glass and crystalline phases to be one order of magnitude smaller than that in the liquid phase ($\eta = 0$). The values for each of the model parameters used in this work are listed in Table II for the $Cu_{50}Zr_{50}$ alloy.

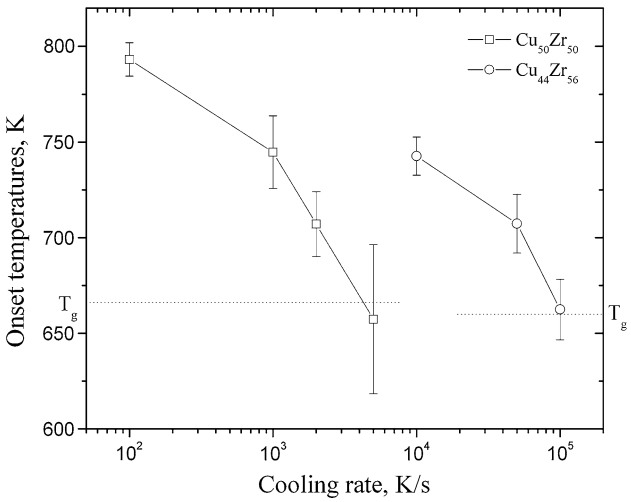

Fig. 4—Phase-field predictions of (crystalline) solidification onset as a function of cooling rate for $Cu_{50}Zr_{50}$ and $Cu_{44}Zr_{56}$ alloys, where the crossover with T_g is the prediction of the critical cooling rate.

B. *Simulation Results*

Examining now the competition between glass formation and crystallization during cooling from the melt, the model reproduces properly a transition in dominance from the crystal solidification to glass formation with increasing cooling rates. The lowest rate for which the crystallization onset is observed is the critical cooling rate for glass formation (R_c). Five runs of simulations were performed for each cooling rate, and the average onset temperatures of crystallization are plotted in Figure 4 with the standard deviations as the error bars. When the onset temperature approaches T_g, the nucleation and growth of crystalline phases will be affected significantly by the glass transition, and different runs of simulations may provide different results. For quenching the liquid $Cu_{50}Zr_{50}$ alloys through T_g with a cooling rate of 5×10^3 K/s (5×10^3 °C/s), two different results were observed from different simulation runs as shown in Figure 5. In run 1, a B2-CuZr particle forms above T_g, and the coexistence of the B2 and glass phases is observed at the final stage. In run 2, nucleation did not occur above T_g, and the crystallization was suppressed completely by the quenching process. To examine the nucleation of the crystalline phases at temperatures below T_g and to get the average onset temperature near T_g, additional simulations were performed in which the glass transition was suppressed artificially. The average onset temperatures summarized in Figure 4 indicate the R_c values of 4×10^3 K/s (4×10^3 °C/s) and 1×10^5 K/s (1×10^5 °C/s) for the alloy compositions of $Cu_{50}Zr_{50}$ and $Cu_{44}Zr_{56}$, respectively. We note also that these values represent the upper bound estimates of R_c because noncrystalline ordering in the liquid, such as the development of extended icosahedral clustering and the emergence of an aggregated network structure, will

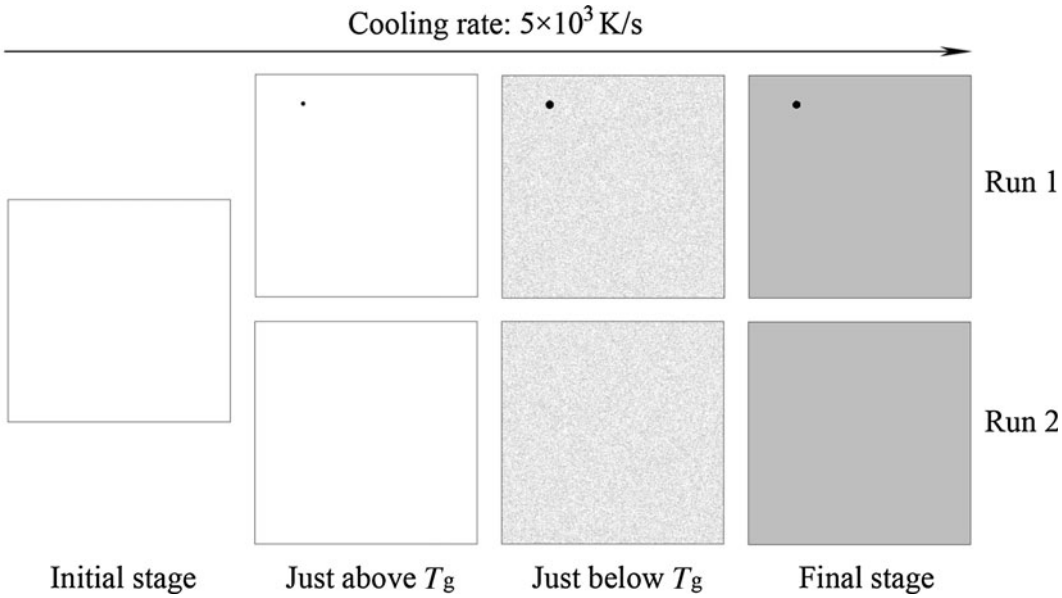

Fig. 5—Simulation results for $Cu_{50}Zr_{50}$ alloys with a cooling rate of 5×10^3 K/s (5×10^3 °C/s). For run 1, the nucleation of the B2-CuZr phase started slightly above T_g, and the coexistence of the B2 (black) and glass (gray) phases was observed. In run 2, the nucleation did not start above T_g, and then the crystallization was suppressed completely.

serve to slow the kinetics of the crystallization process. The R_c values of 2.5×10^2 K/s (2.5×10^2 °C/s)[55] and 4×10^4 K/s (4×10^4 °C/s)[56] have been reported by experimental observations. Taking into account that the experimental measurements may underestimate the R_c values because of the difficulties in identifying small amounts of nanocrystalline material in a specimen, we view our simulation-based upper bound estimates to be consistent with the experimental measurements of R_c. Certainly, however, more rigorous comparisons with experimental observations of crystal/glass competition over a range of cooling rates and alloy compositions are necessary before this type of model can be considered to be generally predictive.

IV. SUMMARY

In the current work, we proposed a combined CF/MPF phase-field approach for describing the phase transformations in glass-forming alloys. The glass transition was treated as a structural relaxation and induced by noise. The competition between the multiple phases was introduced by a MPF treatment. Linking with thermodynamic databases and kinetic information from MD simulations, the proposed model was applied to the Cu-Zr alloys. The competition between the stable and metastable phases was simulated, and the estimated cooling rates were found to be reasonable compared with the reported experimental results. We conclude that this combined CF/MPF method, with additional quantification of critical parameters, may provide a useful means for the simulation-based prediction of glass formation and multiphase structures in glass-forming systems.

ACKNOWLEDGMENTS

This work was supported by the U.S. Department of Energy, Office of Basic Energy Science, Division of Materials Sciences and Engineering. The research was performed at the Ames Laboratory. Ames Laboratory is operated for the U.S. Department of Energy by Iowa State University under Contract No. DE-AC02-07CH11358.

REFERENCES

1. M.I. Mendelev, M.J. Kramer, R.T. Ott, and D.J. Sordelet: *Philos. Mag*., 2009, vol. 89, p. 109.
2. M.I. Mendelev, M.J. Kramer, R.T. Ott, D.J. Sordelet, M.F. Besser, A. Kreyssig, A.I. Goldman, V. Wessels, K.K. Sahu, K.F. Kelton, R.W. Hyers, S. Canepari, and J.R. Rogers: *Philos. Mag*., 2010, vol. 90, p. 3795.
3. S.H. Zhou and R.E. Napolitano: *Acta Mater*., 2010, vol. 58, p. 2186.
4. Z.L. Long, H.Q. Wei, Y.H. Ding, P. Zhang, G.Q. Xie, and A. Inoue: *J. Alloy. Compd*., 2009, vol. 475, p. 207.
5. S. Guo, Z.P. Lu, and C.T. Liu: *Intermetallics*, 2010, vol. 18, p. 883.
6. Z.Y. Suo, K.Q. Qiu, Q.F. Li, J.H. You, Y.L. Ren, and Z.Q. Hu: *Mater. Sci. Eng. A-Struct*., 2010, vol. 528, p. 429.
7. B.S. Dong, S.X. Zhou, D.R. Li, C.W. Lu, F. Guo, X.J. Ni, and Z.C. Lu: *Progr. Nat. Sci.-Mater. Int.,* 2011, vol. 21, p. 164.
8. A. Takeuchi and A. Inoue: *J. Optoelectron. Adv. Mater*., 2004, vol. 6, p. 533.
9. Z.Y. Hou, L.X. Liu, R.S. Liu, Z.A. Tian, and J.G. Wang: *J. Non-Cryst. Solids*., 2011, vol. 357, p. 1430.
10. H.L. Peng, M.Z. Li, W.H. Wang, C.Z. Wang, and K.M. Ho: *Appl. Phys. Lett.,* 2010, vol. 96, p. 021901.
11. S.G. Hao, M.J. Kramer, C.Z. Wang, K.M. Ho, S. Nandi, A. Kreyssig, A.I. Goldman, V. Wessels, K.K. Sahu, K.F. Kelton, R.W. Hyers, S.M. Canepari, and J.R. Rogers: *Phys. Rev. B,* 2009, vol. 79, p. 104206.
12. L. Huang, C.Z. Wang, S.G. Hao, M. J. Kramer, and K.M. Ho: *Phys. Rev. B,* 2010, vol. 81, p. 094118.
13. Y. Dai, J.H. Li, and B.X. Liu: *J. Appl. Phys.,* 2011, vol. 109, p. 053505.
14. O.N. Senkov, D.B. Miracle, E.R. Barney, A.C. Hannon, Y.Q. Cheng, and E. Ma: *Phys. Rev. B,* 2010, vol. 82, p. 104206.
15. X.W. Fang, C.Z. Wang, Y.X. Yao, Z.J. Ding, and K.M. Ho: *Phys. Rev. B,* 2010, vol. 82, p. 184204.
16. S.G. Hao, C.Z. Wang, M.Z. Li, R.E. Napolitano, and K.M. Ho: *Phys. Rev. B,* 2011, vol. 84, p. 064203.
17. J. Berry, K.R. Elder, and M. Grant: *Phys. Rev. E,* 2008, vol. 77.
18. X.D. Hui, X.J. Liu, R. Gao, H.Y. Hou, H.Z. Fang, Z.K. Liu, and G.L. Chen: *Sci. China Ser. G*, 2008, vol. 51, p. 400.
19. W.J. Boettinger, J.A. Warren, C. Beckermann, and A. Karma: *Ann. Rev. Mater. Res*., 2002, vol. 32, p. 163.
20. L.Q. Chen: *Ann. Rev. Mater. Res*., 2002, vol. 32, p. 113.
21. Z.K. Liu, L.Q. Chen, R. Raghavan, Q. Du, J.O. Sofo, S.A. Langer, and C. Wolverton: *J. Comput.-Aided Mater.,* 2004, vol. 11, p. 183.
22. S.G. Fries, B. Boettger, J. Eiken, and I. Steinbach: *Int. J. Mater. Res*., 2009, vol. 100, p. 128.
23. A.G. Khachaturian: *Theory of Structural Transformations in Solids*, Wiley, New York, NY, 1983.
24. L.Q. Chen and W. Yang: *Phys. Rev. B*, 1994, vol. 50, p. 15752.
25. I. Steinbach, F. Pezzolla, B. Nestler, M. Seesselberg, R. Prieler, G.J. Schmitz, and J.L.L. Rezende: *Phys. D*, 1996, vol. 94, p. 135.
26. H. Garcke, B. Nestler, and B. Stoth: *Siam. J. Appl. Math*., 1999, vol. 60, p. 295.
27. W.J. Boettinger and J.A. Warren: *J. Cryst. Growth*, 1999, vol. 200, p. 583.
28. R. Folch and M. Plapp: *Phys. Rev. E,* 2005, vol. 72, p. 011602.
29. T.S. Lo, A. Karma, and M. Plapp: *Phys. Rev. E*. 2001, vol. 63, p. 031504.
30. M. Rappaz, A. Jacot, and W.J. Boettinger: *Metall. Mater. Trans. A*, 2003, vol. 34A, p. 467.
31. S.Y. Hu and L.Q. Chen: *Acta Mater*., 2001, vol. 49, p. 1879.
32. V. Vaithyanathan, C. Wolverton, and L.Q. Chen: *Acta Mater*., 2004, vol. 52, p. 2973.
33. J.Z. Zhu, T. Wang, A.J. Ardell, S.H. Zhou, Z.K. Liu, and L.Q. Chen: *Acta Mater*., 2004, vol. 52, p. 2837.
34. N. Moelans, F. Wendler, and B. Nestler: *Comp. Mater. Sci*., 2009, vol. 46, p. 479.
35. B. Nestler and A.A. Wheeler: *Phys. D*, 2000, vol. 138, p. 114.
36. B. Nestler and A.A. Wheeler: *Comput. Phys. Commun*., 2002, vol. 147, p. 230.
37. B. Nestler, A.A Wheeler, and H. Garcke: *Comp. Mater. Sci*., 2003, vol. 26, p. 111.
38. M. Apel, B. Bottger, J. Rudnizki, P. Schaffnit, and I. Steinbach: *ISIJ Int*., 2009, vol. 49, p. 1024.
39. J.J. Hoyt, M. Asta, and A. Karma: *Mater. Sci. Eng. R*., 2003, vol. 41, p. 121.
40. I. Steinbach: *Model. Simul. Mater. Sci.,* 2009, vol. 17, p. 073001.
41. Y.Z. Wang and J. Li: *Acta Mater*., 2010, vol. 58, p. 1212.
42. S. Kawaguchi and T. Onda: *J. Phys. Soc. Jpn*., 2003, vol. 72, p. 556.
43. P. Bruna, E. Pineda, and D. Crespo: *J. Non-Cryst. Solids*, 2007, vol. 353, p. 1002.
44. M.I. Mendelev, M.J. Kramer, R.T. Ott, D.J. Sordelet, D. Yagodin, and P. Popel: *Philos. Mag*., 2009, vol. 89, p. 967.
45. H.S. Chen: *Rep. Prog. Phys*., 1980, vol. 43, p. 353.
46. K.H.J. Buschow: *J. Appl. Phys*., 1981, vol. 52, p. 3319.
47. W.N. Myung, H.G. Kim, and T. Masumoto: *Mater. Sci. Eng. A-Struct*., 1994, vol. 179, p. 252.

48. N. Mattern, A. Schops, U. Kuhn, J. Acker, O. Khvostikova, and J. Eckert: *J. Non-Cryst. Solids*, 2008, vol. 354, p. 1054.
49. G. Shao: *Intermetallics*, 2003, vol. 11, p. 313.
50. T. Abe, M. Shimono, M. Ode, and H. Onodera: *Acta Mater.*, 2006, vol. 54, p. 909.
51. D. Turnbull: *J. Appl. Phys.*, 1950, vol. 21, p. 1022.
52. D. Turnbull: *J. Chem. Phys.*, 1950, vol. 18, p. 769.
53. L. Granasy, M. Tegze, and A. Ludwig: *Mater. Sci. Eng. A-Struct.*, 1991, vol. 133, p. 577.
54. Y.L. Sun, J. Shen, and A.A. Valladares: *J. Appl. Phys.,* 2009, vol. 106, p. 073520.
55. W.H. Wang, J.J. Lewandowski, and A.L. Greer: *J. Mater. Res.*, 2005, vol. 20, p. 2307.
56. F. Gillessen and D.M. Herlach: *Mater. Sci. Eng.*, 1988, vol. 97, p. 147.